Polymerase Chain Reaction on a Viral Nanoparticle

James Carr-Smith,[#,‡] *Raúl Pacheco-Gómez,*[#,†] *Haydn A. Little,*[‡] *Matthew R. Hicks,*[†] *Sandeep Sandhu,*[†] *Nadja Steinke,*[†,||], *David J. Smith,*[¥] *Alison Rodger,*[¶] *Sarah A. Goodchild,* [§]*Roman A. Lukaszewski,*[§] *James. H. R. Tucker**[‡] *and Timothy R. Dafforn.**[†]

[†]School of Biosciences, [‡]School of Chemistry, [¥] School of Mathematics, University of Birmingham, Edgbaston, Birmingham, West Midlands, B15 2TT, UK.

[¶]Department of Chemistry, University of Warwick, Coventry, Warwickshire, CV4 7AL, UK.

[§]Defence Science and Technology Laboratory, Porton Down, Salisbury, Wiltshire, SP4 0JQ, UK.

KEYWORDS: linear dichroism, nanoparticle, bacteriophage, PCR, shear flow, M13

ABSTRACT

The field of synthetic biology includes studies that aim to develop new materials and devices from biomolecules. In recent years much work has been carried out using a range of biomolecular chassis including α-helical coiled coils, β-sheet amyloids and even viral particles. In this work we show how hybrid bionanoparticles can be produced from a viral M13 bacteriophage scaffold through conjugation to DNA primers that can template a polymerase chain reaction (PCR). This unprecedented example of a PCR on a virus particle has been studied by flow aligned linear dichroism spectroscopy, which gives information on the structure of the product as well as a new prototype methodology for DNA detection. We propose that this demonstration of PCR on the surface of a bionanoparticle is a useful addition to ways in which hybrid assemblies may be constructed using synthetic biology.

INTRODUCTION

An important part of synthetic biology involves harnessing emergent properties of biological building blocks to develop new devices and materials. This includes circuits assembled from genetic control elements, metabolic pathways from enzyme assemblies and assembled materials from peptides, proteins and DNA. Of the latter category, considerable progress has been made in protein-based systems that self-assemble to form a fibrous morphology. For example, design principles have been developed for a number of peptide self-assembly systems based on underlying β-sheet and α-helix architectures. For α-helical structures, coiled-coil assemblies have been used by a number of researchers to design systems with a range of oligomerisation states that are non-fibrous,[1-3] as well as producing systems that can polymerise to form α-helical fibres.[4-6] For β-sheet based structures, the design rules for self-assembly seem less well defined but the fundamental β-sheet amyloid structure has been used extensively as a scaffold for the development of a number of devices. These have included novel cellular scaffolds[7] as well as a range of plasmonic and electronic devices from dipeptides that adopt β-sheet morphologies.[8]

An alternative approach to the construction of materials from biological components has been to exploit an existing fibrous chassis that has been evolved within nature, which concentrates on functionalization of a known scaffold rather than an entirely bottom-up self-assembly process. This approach is well advanced in the case of the M13 bacteriophage chassis, a 1 μm long fibrous particle of helically arranged units made up of a short α-helical peptides (arranged around a DNA core). The particle has the advantage of being easily produced by infection of *E. coli* cultures followed by a simple purification procedure, which yields milligram quantities of dimensionally mono-dispersed particles. The surface of the M13 particle is also easily derivatized *via* two positionally conserved amine functional groups, one on the peptide N-terminus and one on a lysine side chain. These characteristics have been exploited extensively by Belcher and co-workers in producing a wide range of novel materials based on the M13 scaffold. These have included materials for bio-imaging,[9] batteries,[10] and solar cells.[11] In addition Cha and co-workers have used the scaffold to develop novel detection technologies using both antibodies[12] and DNA[13, 14] as affinity tags which can be attached to the M13 surface.

In this paper we show for the first time that a bacteriophage-oligonucleotide conjugate can be used as a reagent in the polymerase chain (PCR) reaction. This provides an entirely new way to direct the assembly of much longer DNA strands onto M13 particles with the potential to form an even wider range of new structures. We also show that the same process can also be used as the basis for a new bioassay system based on linear dichroism (LD) spectroscopy. In 1992 Clack *et al.*[15] first showed that the bacteriophage M13 could be aligned effectively in shear flow, allowing linear dichroism spectra to be measured. LD spectroscopy is a polarised absorbance technique that is only able to produce a signal if chromophores within a scaffold are aligned with respect to one another. The filamentous morphology of M13 means that in solution the particles can be aligned using fluid shear flow. The work of Clack *et al.* not only provided insights into the structure of the particle but also provided the trigger for our own work using M13 as a detection technology. In 2012 we showed that M13 was able to align to an exceptionally high degree in fluid shear flow.[16] We also showed that an M13 particle derivatised with a

pathogen specific antibody could be combined with shear flow induced particle alignment and LD spectroscopy to produce a homogenous assay for the human pathogen *E. coli* O157.[17] The assay relies on the formation of the M13-antibody-pathogen complex perturbing the alignment of the M13 scaffold in shear flow which in turn disrupts its LD signal. In the past three years both Belcher[18] and Cha[13, 14] demonstrated that DNA oligos could be successfully conjugated to the M13 surface. In this work we demonstrate for the first time that PCR can be used to extend the DNA on the M13 surface, leading to a perturbation in alignment and hence a change in the LD signal.

Overall the work presented here demonstrates two principles. Firstly that PCR can be used in conjunction with oligonucleotide labeled M13 to provide a new hybrid bio-nanoparticle; this has the potential to provide an extra tool for building higher order assemblies of M13 for broader synthetic biology applications. Secondly we demonstrate that M13-DNA conjugates can be used as the basis for a DNA assay system that could be used *e.g.* in combination with our immune-assay system to provide a multimodal sensing device.

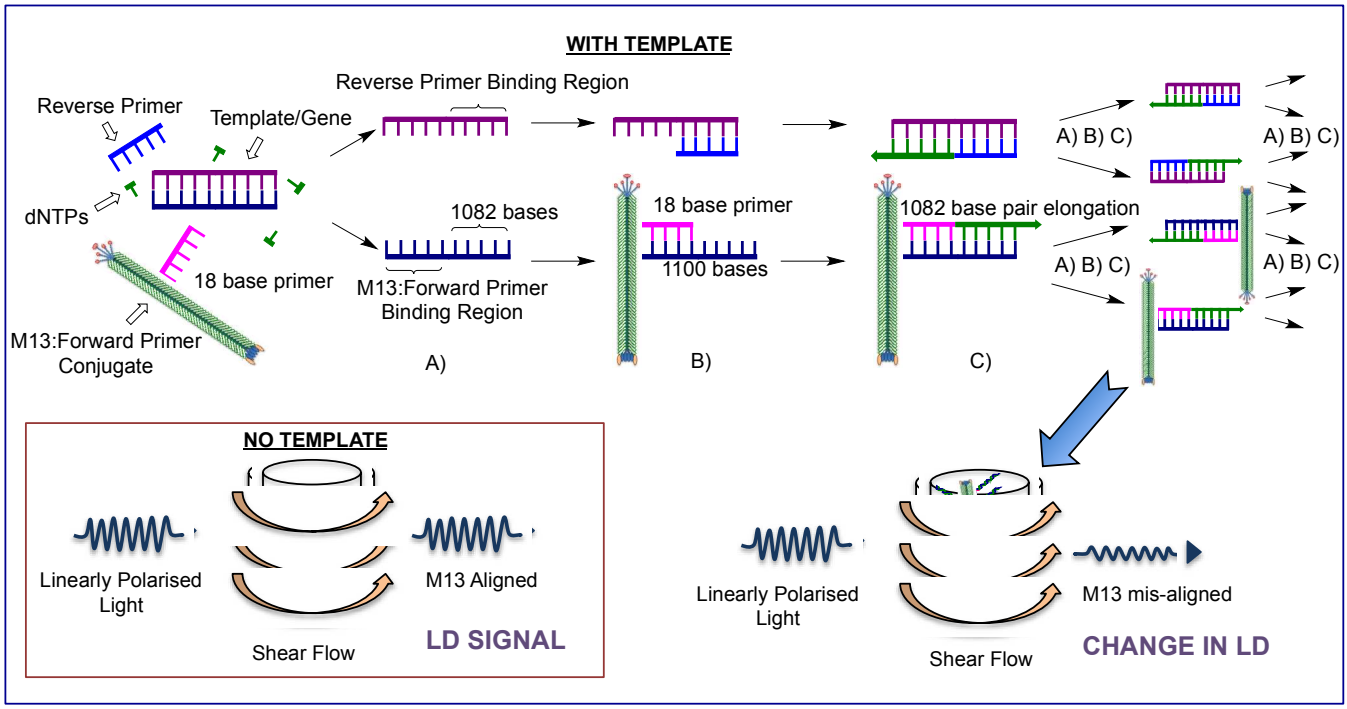

Figure 1. Diagrammatic representation of the rationale behind PCR on a virus nanoparticle and detection using linear dichroism. The M13-bacteriophage is conjugated to DNA oligonucleotides primers that can partake in sequence specific polymerase chain reactions, replacing standard primers. A) denaturing B) annealing C) extension. Following amplification the presence of pathogen/template is detected by changes in changes in M13 virus nanoparticle alignment in shear flow.

RESULTS AND DISCUSSION

Primer Design The several components were designed as follows. An 18-mer primer (**R-For**, Table 1) was synthesised containing a C6 disulfide (SS) tagged at its 5'- end, which was subsequently cleaved by reduction with TCEP to leave a reactive thiol for conjugation to the protein surface of the virus.[13, 14, 18] Its base sequence was chosen to allow the synthesis of the *ampR* gene from its 5' end by PCR. However, to test whether such a derivatisation had been successful, a simple spectroscopic method was required to quantify the number of DNA strands that had been attached to the viral scaffold. Therefore a fluorescent chromophore label, carboxytetramethylrhodamine dye TAMRA-dT, was also incorporated. Furthermore, two other oligonucleotides were also prepared containing fluorophores, one was a sequence complementary to the primer (**F-Com**) and the other a random sequence (**F-Ran**), which were both labeled with fluorescein (6-FAM). These modifications were designed so that fluorescence anisotropy could be used to assess whether the **R-For** primer strand was still able to form a duplex when conjugated to the M13 bacteriophage.

Table 1. Sequences of the synthesized oligonucleotides.

Name	Sequence (5'-3')
R-For	SSC_6-(TAMRA-dT)ATGAGTATTCAACATTTC
F-Com	(6-FAM)- GAA ATGTTGAATACTCAT
F-Ran	(6-FAM)-TCATCAGTCAGTCAGTCA

The DNA strand **R-For** was conjugated to the pVIII major coat protein of the M13 bacteriophage using a two-step reaction (Scheme 1) in which the pVIII (of which there are approximately 2700 copies)

was first chemically modified to incorporate a maleimide group provided by SMCC. SMCC can form a stable amide bond between the amine groups of the pVIII protein and the NHS-ester in the SMCC,[19, 20] leaving a maleimide group free to react with thiol groups.

We assume that the better solvent accessibility and lower pK_a value of the N-terminus compared to the lysine residue makes it the preferential group for reaction with the NHS-ester.[21] Once the pVIII protein was derivatised with SMCC, **R-For** was then added for conjugation to the M13 via thioether bond formation. The bacteriophage material was then separated from the unreacted components using size exclusion chromatography. Figure 2a shows the elution chromatogram of the desired material at the expected position for the M13, which gave an absorbance at two different wavelengths; 269 nm and λ_2 = 280 nm (providing a combined signal from the M13 bacteriophage and the base-pairs in the conjugated residues within the major coat protein pVIII). Additionally an absorbance at λ_3 = 555 nm, which provides a specific signal for the rhodamine dye TAMRA incorporated into the oligo, and hence the oligo itself, was monitored throughout. Other materials that eluted after the main band were ascribed to unreacted DNA and small molecules such as glycine and TCEP, which were used during conjugation process.

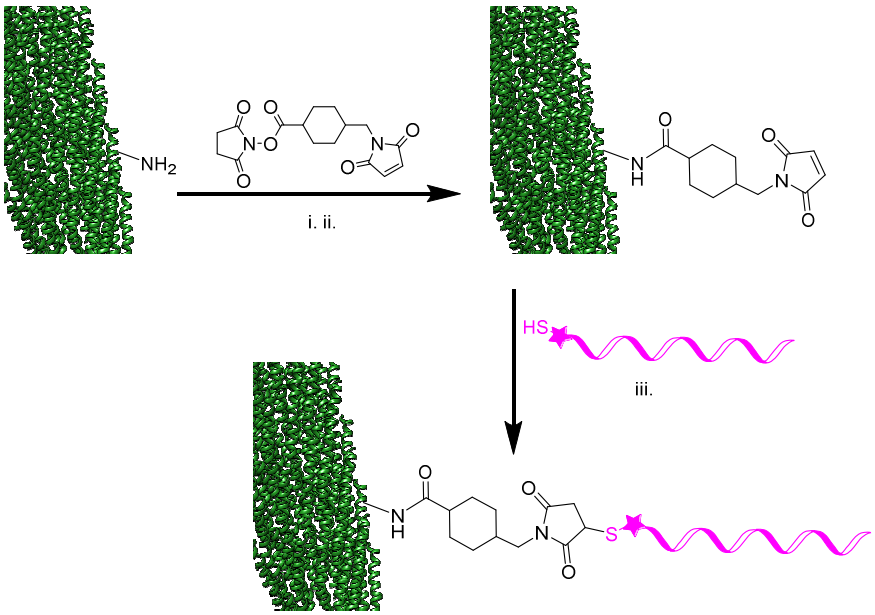

*Scheme 1. A two-step bioconjugation of **R-For** DNA to the pVIII protein of wtM13 bacteriophage via a heterobifunctional SMCC linkage. i) SMCC in DMSO, 1 hr, RT. ii) glycine, 15 min, RT. iii) **R-For** (star denotes TAMRA dye) in its reduced thiol form by addition of TCEP, 16 hrs, 5 ^{o}C*

Fractions from the size exclusion purification containing the modified bacteriophage were then analysed using UV-Vis absorbance spectroscopy to determine the conjugation efficiency. Measurement of the TAMRA signal at 555 nm allowed for quantification of oligonucleotides appended to each particle (see Figure S5). These data show that approximately 0.3% of the pVIII proteins in the M13 coat had been conjugated to **R-For**, which equates to an average of *ca.* 8 oligos per particle (assuming 2700 pVIII proteins per M13 bacteriophage). The low yield is not unexpected as the reaction mixture contained only enough DNA to label 4% of pVIII proteins, so that the actual yield of the reaction was 8%. Although this is a relatively low loading, we consciously took a conservative approach to M13 conjugation based on our experience with other M13 conjugation experiments. These have shown that in some cases (notably when large molecules such as proteins are conjugated to M13) higher levels of conjugation lead to unwanted disruption of M13 alignment in flow, either through aggregation or disruption of the M13 structure. Below 10% represented a safe region for antibody conjugated M13 and therefore these experimental conditions were chosen for this experiment. Further evidence for the successful conjugation of **R-For** to the bacteriophage came from fluorescence anisotropy experiments (*vide infra*) as well as SDS PAGE analysis of the pVIII protein (Figure 2b). Denaturation of the virus particle and subsequent separation showed an additional protein band at *ca.* 12 kDa, indicative of an increase in molecular weight of 6.7 kDa from the appended oligonucleotide **R-For.**

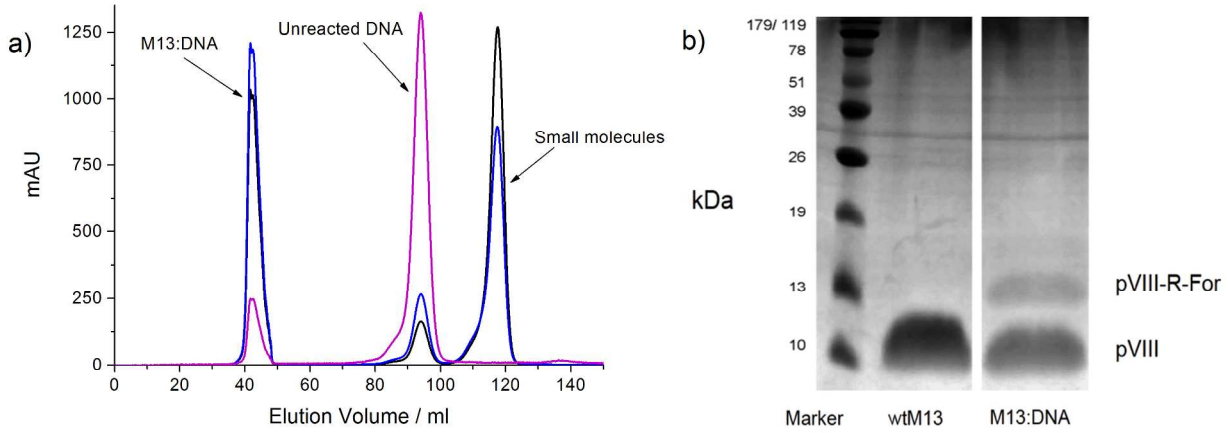

*Figure 2. Purification and characterization of the M13-**R-For** bioconjugate. a) Size exclusion chromatogram of the conjugate mixture monitored at three wavelengths; 269 nm (blue line), 280 nm (black line) and 555 nm (pink line). b) SDS PAGE comparing the pVIII protein of M13 and the M13-**R-For** conjugate after purification (an unedited version is included in the supplementary material as S4).*

One of the two aims of this project was to produce a DNA detection system where the presence of target DNA was detected by the formation of an extended amplimer on the surface of the M13 which would lead to an alteration in the LD signal. This meant that it was key that the conjugation of the DNA primers to the M13 did not drastically effect the alignment of the M13 in flow and hence the LD signal of the particle. Micron and sub-micron-sized particles such as M13 tumble in fluid under rotational Brownian motion and Couette flow produces an LD signal by biasing the orientation distribution towards the flow direction, which can be quantified via the rotational Peclet number.[22] Intuitively, this biasing can be understood as arising from the lesser shear moment exerted by the flow on a molecule aligned in the flow direction compared with one aligned in the direction of the velocity gradient. In the Couette device, the flow direction is azimuthal; the velocity gradient is radial, resulting in a bias towards azimuthal alignment (Figure 1). Given the reliance of the alignment of the M13 on shape it is possible that additions to the surface of the bacteriophage could alter the hydrodynamic behavior to prevent alignment in shear flow and hence disrupt measurement of the LD signal. M13 bacteriophage displays a distinct LD spectrum (Figure 3 – solid line) indicative of various transitions within the particle's aligned structure.[15, 17] Positive bands in the far UV-visible (below 240 nm) and at 270-310 nm are the result of

π-π* transitions and tyrosine and tryptophan absorbances respectively, with their sign due to the parallel orientation axis of peptide backbones with respect to the axis of the particle itself. A negative band between 240 and 260 nm results from the perpendicular orientation of viral DNA base pairs with respect to the M13 particle. Following conjugation, these characteristic bands are still observed as unperturbed transitions that display the correct sign. This indicates that conjugation of short primers to the major coat protein of M13 does not alter the structure in a way that affects its alignment in shear flow. This observation is perhaps not surprising as the single stranded primers would be less than 6 nm in length (18 bases × 0.33 nm), which represents a relatively minor addition to the M13 structure (given that M13 is almost 1 μm in length). When this is combined with the low conjugation number (8 oligonucleotides per M13), it is very unlikely that the alignment, and hence LD signal of the M13, would be affected by primer conjugation.

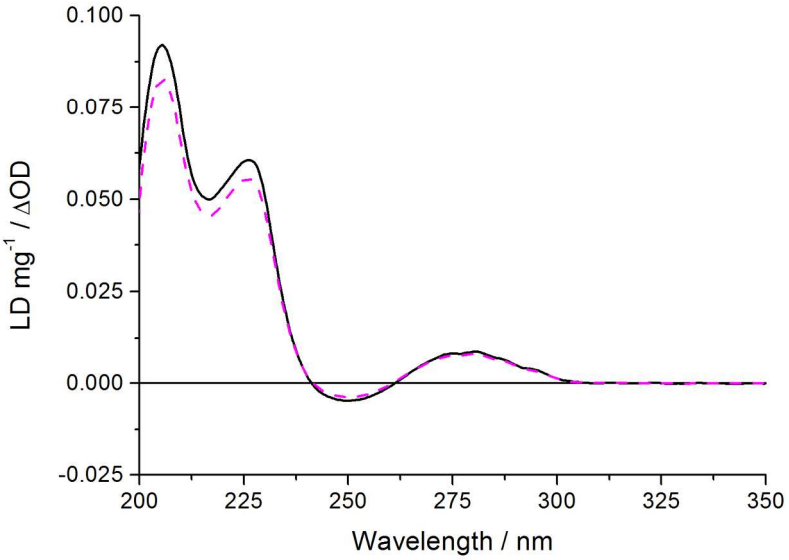

*Figure 3. A comparison of the alignment of wtM13 (solid black line) and M13-**R-For** (pink dashed line) in shear flow using LD spectroscopy. 50 mM potassium phosphate buffer pH 8, 150 mM NaCl. Couette flow 3000 rpm*

Lee *et al.* have previously shown that duplex formation between short oligonucleotides (15 base pairs) was not disrupted by the conjugation of M13 to one DNA strand.[14] In a similar fashion, we could also readily demonstrate that duplex formation between M13:**R-For** and **F-Com** was possible using

fluorescence anisotropy (FA), a technique that signals changes in motions of a fluorophore upon interaction with another species. The FA of the rhodamine moiety was indeed higher (0.128 ± 0.0006) when attached to M13 than when free (0.061 ± 0.002), which was consistent with its attachment to the much larger M13 viral coat. Furthermore, Figure 4 shows an increase in FA of the fluorescein chromophore in **F-Com** upon addition of the complementary M13:**R-For**. Importantly, a similar effect was not observed when the non-complementary strand **F-Ran** was used instead of **F-Com**, or when unfunctionalised M13 (wtM13) was added instead of M13:**R-For**, proving that duplex formation between the complementary strands was responsible for the increase in the signal. In fact, dependence of the FA of **F-Com** on the concentration of the M13-DNA conjugate shows that a maximum signal is reached at a molar ratio of 1:1. It is worth noting that this change in FA is not likely to be the result of a change in overall complex size and hence tumbling time of the complex caused by the binding of the relatively small **F-Com oligo** to the much larger M13-DNA conjugate (*ca.* 1 micron in length). This is because the lifetime of the probes used (fluorescein has a lifetime of 4 ns while tetramethyl rhodamine has a lifetime of 2 ns) is too short to report the motions of such a large complex. Instead the observed anisotropy signal is more likely to be the result of a change in more rapid molecular motions occurring within the DNA structure close to the fluorophore. In other words, not surprisingly it appears that DNA base pairing interaction arising from duplex formation dampens the motion of the fluorophore.

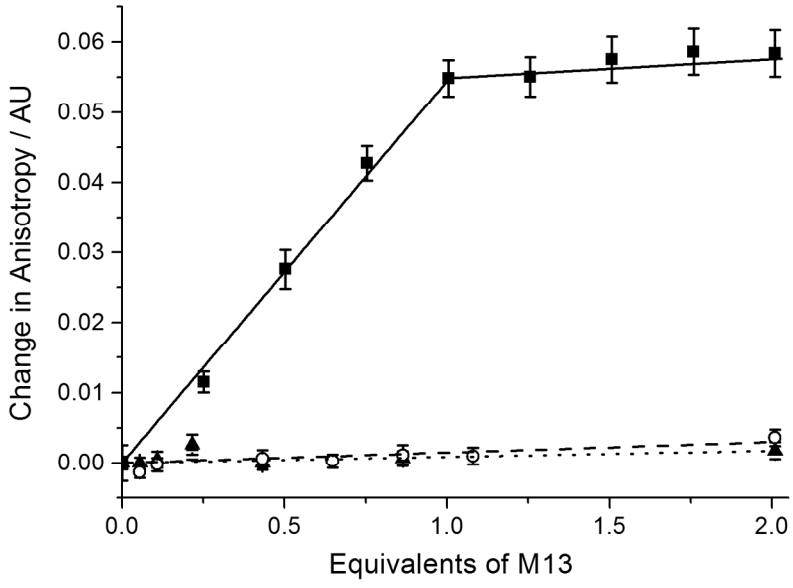

Figure 4. Fluorescence anisotropy changes upon addition of target M13DNA conjugates or wtM13. M13-R-For + F-Ran (circles), wtM13 + F-Com (triangles) and M13-R-For + F-Com (squares). 25 nm DNA, 150 mM NaCl, 50 mM potassium phosphate buffer pH 8.0. Error bars represent the S.E.M of a minimum of 3 repeats.

In agreement with the anisotropy change observed for duplex formation with **R-For** on the M13, a similar change in FA was observed for the control reaction where unconjugated **R-For** was added to **F-Com** (Fig S6, Supplementary Info.). Together these data show that conjugation of the **R-For** primer to the surface of the M13 does not affect its ability to bind to complementary DNA sequences.

An essential part of the cyclic process underlying the PCR reaction is the thermal denaturation step. This step, which is usually carried out at ~ 94^{o}C, induces double stranded amplimers in the reaction solution to dissociate, which subsequently allows the binding of more primers once the temperature is lowered (the denaturing and annealing steps in Fig. 1 respectively). In general, sustained incubations of proteins at elevated temperatures, like those used in the PCR, lead to aggregation of the protein and a loss of activity. These elevated temperatures could also lead to aggregation of M13, preventing alignment and eliminating the LD signal. It was therefore important to assess whether M13 could resist prolonged incubations at elevated temperatures. LD spectroscopy provides an excellent measure of structural integrity of the M13, as the signal is directly linked to the structure of these long particles. The results of this study are illustrated in Figure 5, which shows the LD spectra and signals for samples of M13 incubated for 1 minute at various temperatures. These data show that the LD signals, and hence the structure of M13, diminishes considerably above 86^{o}C.

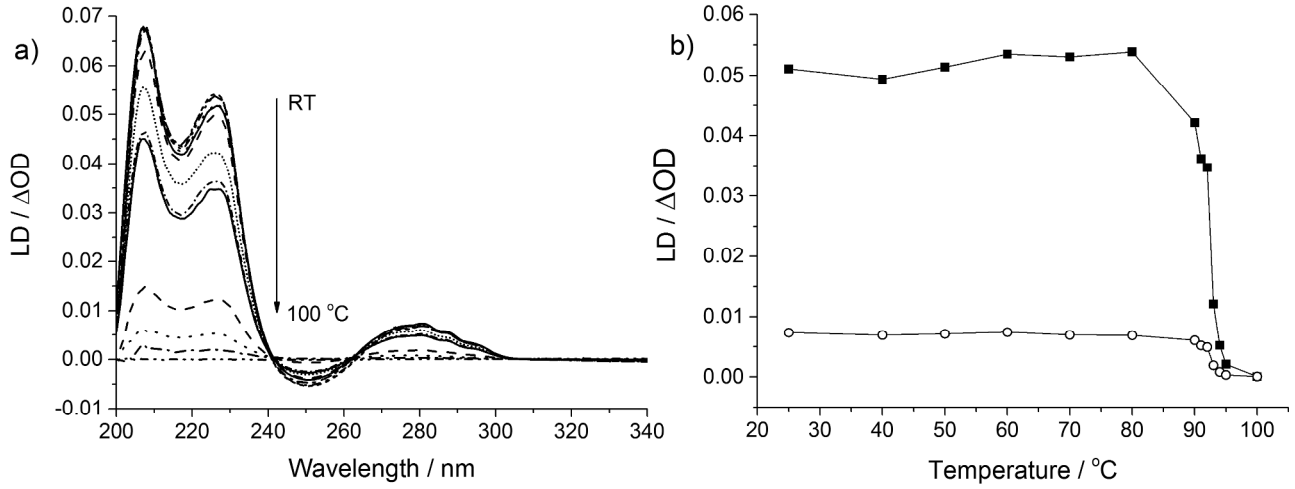

Figure 5. a) Effect on M13 stability and hence LD upon incubation with increasing temperatures for 1 minute. As the temperature increases the intensities of the LD spectra diminish. b) This effect is seen more clearly by examining the change in LD intensity at a single wavelength with respect to temperature; 225 nm (squares), providing information on changes in peptide backbone alignment and 280 nm (circles), providing information on aromatic side chain alignment. M13 concentration = 0.11 mg/ml.

These observations indicated that PCR using LD spectroscopy and M13 could only be carried out using denaturation temperatures that were not in excess of 86^{o}C. This was confirmed by subjecting the conjugated bacteriophage M13:**R-For** to 35 simulated (i.e. in the absence of any template) PCR thermocycles at a range of different denaturation temperatures (Figure 6). These revealed that as expected there was a marked loss in the M13 LD signal above 86^{o}C,

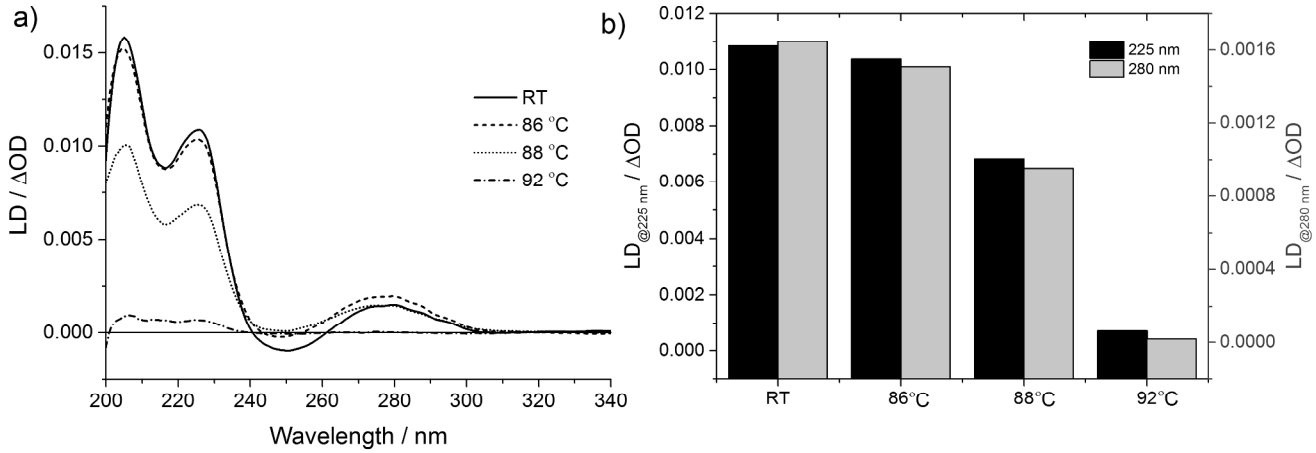

Figure 6. a) LD spectra showing M13 alignment following 35 simulated PCR cycles in the presence of standard PCR reagents (but no template) at various temperatures. b) LD signal at two different wavelengths (225 nm – black and 280 nm – grey) taken from the LD spectra shown in a). M13 concentration = 0.024 mg/ml.

Given the thermal stability results described above, PCR studies over 35 cycles were next carried out to assess the requirement for a 94ºC denaturation step in the presence of *ampR* (i.e. the DNA target gene that acts as the template) at a concentration of 2 ng/µl (Fig S8, Supplementary Information). These data importantly revealed that the PCR could still proceed and produce the desired amplimer at the lower temperature of 86ºC in the presence of ethylene glycol using unconjugated primers **R-For** and the commercially available reverse primer (see lane 2, Figure 7). Furthermore, we were then able to successfully demonstrate that the PCR could also proceed under these conditions using M13:**R-For** as the forward primer, as shown in Figure 7, Lane 3.

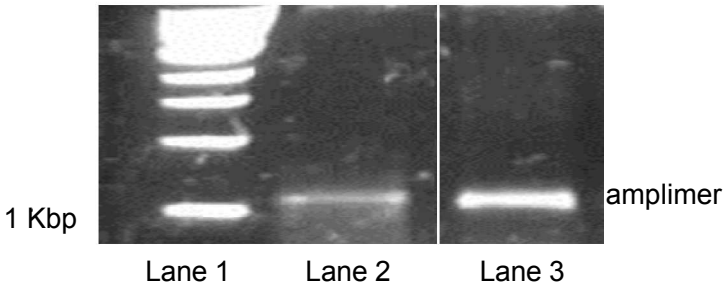

*Figure 7. Agarose gel indicating the success of PCR amplification at 86°C using standard forward and reverse primers (Lane 2) over 35 cycles. Successful amplification of the ampR gene is also observed when the forward primer is replaced with **M13-R-For** at the same temperature (Lane 3). A 1 kbp DNA ladder is also shown (Lane 1)*

One of the central premises of this study is that M13-primer conjugates can be used in combination with flow-aligned linear dichroism spectroscopy to provide a new method for DNA detection using PCR technology. To induce a change in the LD signal of the M13, the amplimers of the ampicillin resistance gene (*ampR*) formed in the PCR (which are hence attached to the M13 particle) have to disrupt the

alignment of the M13. To examine whether this is theoretically likely, the structure of the end product of the PCR needs to be considered. The number of the attached amplimers can be calculated if we assume that all primers on the surface have been extended out by the PCR. This would mean on average eight amplimers of *ca.* 1 kb length on the surface of each M13. A DNA fragment would form approximately a 0.35 μm long protrusion on the side of the M13, which itself is approximately 1 μm in length. The question therefore remained whether the presence of 8 amplimers (each *ca.* 0.35 μm in length compared to ~ 6 nm for the primers) on the surface of M13 was enough to alter the alignment of the M13 and hence the LD signal. To test this, LD spectra of the end product of the PCR performed at 86ºC over 35 cycles using the M13:**R-For** conjugate were recorded (See Figure 8). It was very interesting to note that the full spectral data revealed a dramatic change, giving what is essentially an *inverted LD signal* for the phage after the PCR in the presence of the template (Figure 8a – blue line) compared to that after a simulated PCR under the same conditions in the absence of the template (Figure 8b - red line). The measurements included a number of important control experiments, including the effect of the PCR thermo-cycling process on the LD the signal of the M13:**R-For (**Figure 8b A and C**,** carried out in the absence of the DNA target). Another control experiment was a measurement of the LD signal for the PCR carried out using conventional (e.g. without conjugated dyes) primers rather than M13:**R-For** (Figure 8b- sample B) to ensure that the signal changes were not the result of any contaminating unconjugated primers producing DNA amplimers. This was an important consideration, as we have previously shown that simple DNA amplimers alone, albeit at much higher concentrations, give a negative LD signal,[23] which could alter the observed signal from the M13. Success in these controls has allowed us to unambiguously demonstrate that PCR amplification of the DNA target *ampR* on the surface of the M13 bacteriophage can be measured using LD spectroscopy. These data fit with the expected effect of the formation of amplimers on the viral surface. These disrupt the fibre like structure of the M13 and hence its flow alignment and LD signal intensity. However the observed LD signal change has exceeded the initial expectations of this work in that instead of the LD signal from the conjugated phage simply reducing to zero upon gene amplification, an inverted spectrum is observed

(Figure 8). This indicates that the addition of amplimers to the M13 surface has altered its shape in such a way that results in an effect that is more profound than a simpler lowering of particle alignment. Instead alignment remains but the formation of eight 1kb long duplexes on the particle alters its axis in a way that leads to a signal inversion (Figure 9).

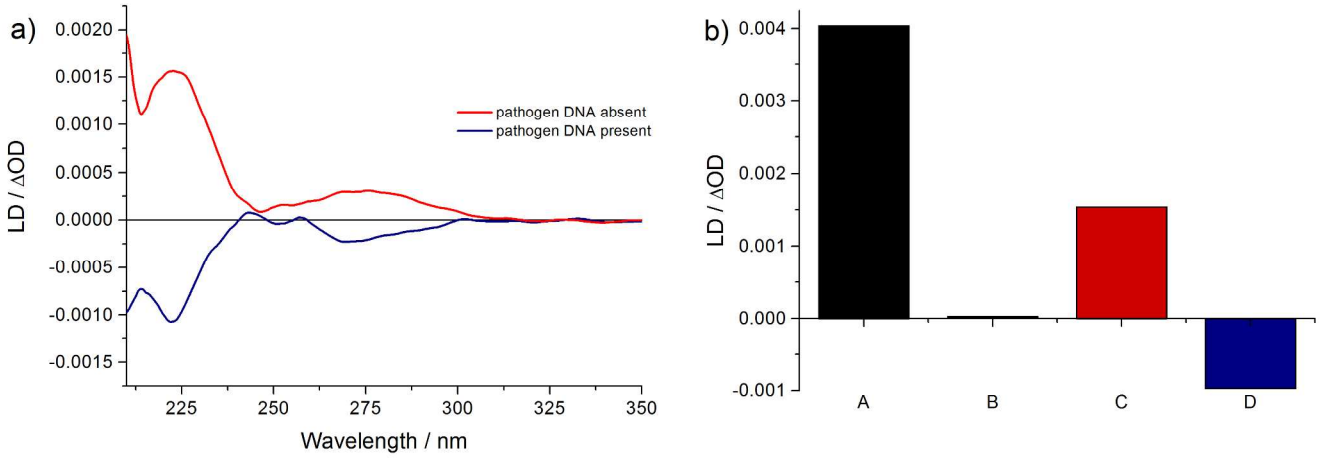

*Figure 8. (a) Comparison of the LD spectra from PCR cycles (annealing temperature 86*ºC, 35 cycles) *using M13:**R-For** as the forward primer in the absence (red line) and presence (blue line) of the ampR template (pathogen) at room temperature. Spectra were subjected to a 75 point Savitsky-Golay smoothing function. (b) The observed LD signals at 225 nm using **M13-R-For** in the absence (C) and presence (D) of template. The LD signals at 225 nm with no PCR cycles using **M13-R-For** in the presence of template (A) and from a PCR reaction using conventional **R-For** as the forward primer (B) are also shown. **M13-R-For** concentration = 0.012 mg/ml.*

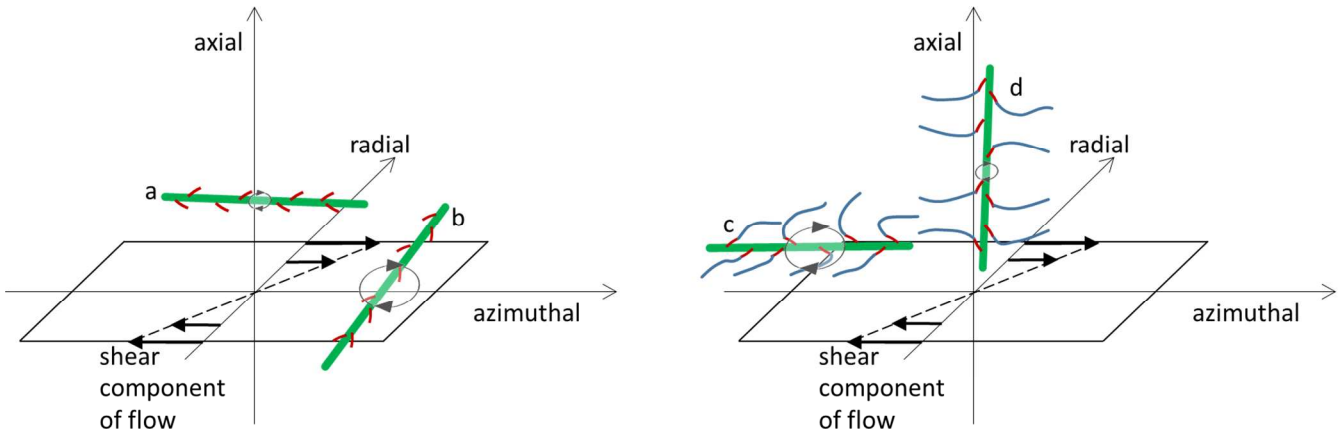

Figure 9. Schematic model of M13 bacteriophage behaviour in shear flow following PCR in the absence (a,b) and presence (c,d) of ampR, showing the shear component of the flow and principal axes. M13 is depicted as a green rod, with primers in red and amplimers in blue.

CONCLUSION

Different classes of biomolecule have quite different characteristics. Proteins for example are able to form complex globular structures that are ideally suited to functions as diverse as catalysis and signal transduction. Proteins can also participate in high order associations to produce large-scale particles with significant structural integrity, with perhaps some of the best examples of this being viral capsids. However in the latter case, unraveling the "molecular code" that drives such associations still eludes us in all but the simplest cases. DNA in comparison has a very simple assembly code, which can be readily used to design and assemble highly complex structures. The aim of the work detailed here was to explore a method to link a structural element, namely the bacteriophage M13, to an easily programmed assembly element, DNA. Previous work had shown that small oligonucleotides could be attached to the surface of M13. However progress in this endeavor had stalled when the desire for larger pieces of DNA required far more complex assemblies. To address this issue, we turned to PCR using bacteriophage-conjugated primers to allow much longer pieces of DNA to be synthesized *in situ* and simultaneously attached to the viral chassis. Thus, we have provided a simple method for generating hybrid nanoparticles that contain extended DNA assembly sequences.

In achieving this aim we have shown for the first time that an M13-oligonucleotide conjugate can participate in a PCR by acting as a primer, yielding a 1kbp long amplified gene product attached to the coat of the bacteriophage. We have confirmed the presence of this product by changes in hydrodynamic behavior of the virus particle, by band shifts on agarose gel electrophoresis, and by perturbation of the flow aligned LD spectrum. From this we have demonstrated that the change in LD spectrum offers a

quick read-out method that can be used in future experiments to explore the production of these DNA-M13 hybrid structures.

We also propose that the change in LD signal induced by amplimer production could underpin a novel DNA detection system. The formation of the DNA-M13 complex results in an inversion of LD signal when compared to the M13 prior to the PCR reaction. This observation has two important consequences. Firstly it shows that the structure formed by the DNA-bacteriophage forms a defined structure with different hydrodynamic properties and hence alignment in shear flow. Secondly it increases the dynamic range of an LD assay based on this methodology, leading to an improvement in sensitivity.

One question however, does remain; why does the LD signal invert? This may be explained by examining the origin of the signals more closely. The work of Clack[15] indicates that the LD signal is produced by the long axis of α-helix that makes up the major pVIII protein in the viral coat being oriented 20^{o} from the long axis of the viral particle. The intensity and sign of the LD signal is related to the cos^2 of the angle between relevant electronic transition and the alignment axis.[24] This means that if the particle is aligned at 54.7^{o}, the transition will exhibit no LD. However if the angle is less than 54.7^{o}, the signal is positive (as we observe in the M13 starting material). But if the angle is greater than 54.7^{o}, then the signal becomes negative (as we observe at the end of the PCR reaction). Given that the angle of the major M13 chromophore to the alignment axis is 20^{o} when not cross-linked, then all that would be required for a change in signal sign is a movement of more than 34.7^{o} away from the alignment axis.

An understanding how this alignment change could be induced can be gained by a more careful consideration of how the M13 aligns in shear flow. In the absence of pathogen DNA, an M13 bacteriophage fibre instantaneously pointing in the flow (azimuthal) direction is minimally affected by shear compared with when it is pointing in the direction of the velocity gradient (Figure 9a, b). This difference biases the orientation distribution of the Brownian M13 fibres azimuthally; this bias underlies the production of the LD signal. In the presence of pathogen DNA and following PCR, the amplimers increase the rotational drag profile of an M13 fibre pointing in the flow direction, tending to cause the

tumbling and thereby disrupting the tendency of fibres to align in the flow direction (Figure 9c). However, an M13 fibre pointing in the axial direction is subject to a new effect: the smaller amplimers will tend to extend from the M13 'backbone' and align in the flow direction, stabilising the M13 in this configuration (Figure 9d). We hypothesise that the overall effect of the amplimers is to bias the orientation distribution in the axial direction, reversing the LD signal. Elongated bodies in viscous flow with such protruding 'hairs' can have dramatically altered hydrodynamic properties, as for example in the hispid flagella of *Ochromonas malhamensis,*[25] the presence of these hairs inverts the typical axial/normal drag anisotropy of the slender flagellum, reversing the swimming direction when compared with smooth flagellates.[26]

In summary, we have shown an unprecedented example of a PCR carried out on the surface of a virus nanoparticle. Not only has this process produced a new hybrid DNA-viral particle for future use in the design of extended DNA assemblies, it also provides a novel PCR-based DNA detection methodology. This could be combined with previous work on M13 immunoassay-based detection, to provide a potential route for multiplexed and multimodal assays.

METHODS

Materials. Chemical reagents were all purchased from Sigma-Aldrich (Gillingham, UK) and used as received without further purification unless otherwise stated.

All DNA synthesis reagents and materials were purchased from Link Technologies (Bellshill, Scotland) unless otherwise stated. Reagents were used as received without further purification and unless otherwise stated used according to the manufacturer's recommendations.

Growth and Purification of Wild-type M13 (wtM13). Wild-type M13 bacteriophage (wtM13) was produced by inoculating *E. coli* Top 10 F' using the method detailed previously.[17] To purify the M13 bacteriophage the material recovered from the first round of purification was subjected to a further purification using caesium chloride gradient centrifugation. M13 bacteriophage was mixed with CsCl powder to give a final concentration of 0.4 mg/mL of CsCl. The samples were centrifuged for 24 hours at 35,000 rpm in a 70.1 Ti rotor at 15 °C. This resulted in the formation of a diffuse band containing M13 bacteriophage. The band was extracted and the samples were dialysed in 50 mM potassium phosphate buffer pH 8.0 with 3 changes of 1 L each.

M13 Conjugation of Bifunctional Linkage. An initial mass of 2 mg (1.1×10^{-10} moles) of CsCl purified wtM13 bacteriophage was adjusted to a final volume of 1 ml by adding 0.1 M potassium phosphate buffer, pH 7.5 in a micro-centrifuge tube. 1.056 mg (3.16×10^{-6} moles) of SMCC (succinimidyl-4-(N-maleimidomethyl)cyclohexane-1-carboxylate, Thermo Scientific Pierce) was dissolved in 10 μL DMSO and added to the mixture to provide a 10:1 molar excess over the M13 bacteriophage pVIII protein (it is assumed that there are 2700 pVIII proteins per M13 particle). The sample was then incubated for 1 hour at room temperature, before being quenched with 0.23 mg (3.16×10^{-6} moles) of glycine for 30 minutes at room temperature. The maleimide-derivatised product was then separated from low molecular mass by-products using a PD-10 column (Sephadex G-25, GE

Healthcare). The sample was eluted in conjugation buffer (50 mM potassium phosphate buffer, 150 mM NaCl, 5 mM EDTA, pH 7.0).

Oligonucleotide Synthesis, Purification and Characterisation. Synthesis of the rhodamine labeled forward primer (**R-For**) 5'-SSC_6-(dT-carboxy tetramethyl-rhodamine)-ATG AGT ATT CAA CAT TTC-3', complementary sequence (**F-Com**) 5'-(6-FAM)- GAA ATG TTG AAT ACT CAT-3' and complete mismatch (**F-Ran**) 5'-(6-FAM)-TCA TCA GTC AGT CAG TCA-3' was carried out on an Applied Biosystems 394 DNA/RNA synthesiser (Foster City, California). ULTRA-mild DNA synthesis conditions were used for the synthesis of fluorophore labeled oligonucleotides in which the use of Pac-dA-CE, Ac-dC-CE and iPr-Pac-dG-CE phosphoramadites was required. Cleavage from CPG column was carried out using 0.05 M potassium carbonate solution at RT for 4 hours. Labeling of oligonucleotides with a 5' thiol (SSC_6) was achieved *via* a commercially available C6 trityl protected thiol phosphoramidite (Glen Research, Virginia, USA). Fluorophore labeling with carboxy tetramethyl-rhodamine(TAMRA)-dt and 6-Carboxyfluorescein(FAM) was achieved via commercially available phosphoramadites (Glen Research). Purification and characterisation was carried out as previously described.[27] Disulfide labeled oligonucleotides were deprotected according to manufacturer's instructions and subsequently desalted for a second time using a NAP-10 column. The disulfide labeled oligonucleotides were then reacted with 50 mM tris(2-carboxyethyl)phosphine (TCEP) for 30 minutes prior to bioconjugation. Analytical HPLC traces and mass spectra of the purified oligonucleotides can be found in the supporting information (Figures S1-S3).

Bioconjugation. 11.7 μL of 1 mM (1.17×10^{-8} moles) thiol labeled oligonucleotide in conjugation buffer (50 mM potassium phosphate buffer, 150 mM NaCl, 5 mM EDTA, pH 7.0) was added to the SMCC labeled M13. The solution was mixed and left to react at RT for 1 hour before gentle stirring at 5 ^{o}C overnight. 14.6 μL of a 10 mg/ml (1.17×10^{-7} moles) solution of N-ethylmaleimide (NEM) in conjugation buffer was then added to the mixture, stirred and left to react at RT for 15 minutes and finally purified by size exclusion chromatography.

Size Exclusion Chromatography. M13-oligonucleotide conjugates were purified using an ÄKTA Explorer 10 purification system (GE Healthcare), fitted with a Superdex 200 (120 mL column volume) HiLoad 16/60 prepacked column. The column was equilibrated with 1 column volume of water and 1.2 column volumes of buffer (50 mM potassium phosphate buffer and 150 mM NaCl, pH 8.0) before sample injection. Three wavelengths were recorded simultaneously: λ_1 = 269 nm, λ_2 = 280 nm and λ_3 = 556 nm. 2 mL fractions were collected using a Frac-950 fraction collector (Amersham Pharmacia Biotech).

SDS PAGE. Samples were run vertically on a 12% SDS Page denaturing gel. A 20 μL sample (0.8 mg/ml M13) in loading buffer (Tris, glycerol, β-mercaptoehanol) was first denatured at 95 ^{o}C for 15 minutes before loading into the wells. The gel was run for 40 minutes at 200 V (400 mA) before staining with Coomassie Blue for 1 hour, and subsequently destained using a 3× solution of acetic acid in MeOH for 1 hour. The resulting gel was then visualised on a light box.

Measurement of M13/DNA Concentration. Absorption spectra to determine bacteriophage concentrations for LD experiments using the method previously detailed,[17] were carried out using a JASCO V550 UV/Vis spectrometer. DNA concentrations and conjugation efficiencies were calculated using the observed absorbances for DNA (**R-For**) ($\varepsilon_{260\ nm}$=187,000 M^{-1} cm^{-1}), rhodamine ($\varepsilon_{556\ nm}$=129,000 M^{-1} cm^{-1}) and fluorescein ($\varepsilon_{495\ nm}$= 75,000 M^{-1} cm^{-1}).

Measurement of LD Spectra. Measurements were performed on a Jasco J-715 Spectropolarimeter (Jasco, Japan) which has been modified to measure linear dichroism. The samples were placed into a micro-Couette cell housed in the Jasco J-715. LD spectra were recorded at room temperature over a wavelength range from 350−190 nm at a scan speed of 100 nm/min, with a 0.2 nm data pitch, 2.0 nm band width and 1 sec response time. Couette flow was generated through a rotation at 3000 rpm. For each experiment, a baseline (non-rotating capillary) was collected, subtracted from the rotating spectrum and the signal was subsequently zeroed at 350 nm.

Fluorescence Measurements. Fluorescence spectroscopy measurements of M13-oligonucleotides were performed in buffer (50 mM potassium phosphate and 150 mM NaCl, pH 8.0) using a LS 50B fluorescence spectrometer (Perkin Elmer) and a three-window fluorimeter sub-micro cuvette (Starna) with a 3 mm pathlength and a 45 μL nominal volume. All studies were performed at room temperature. Samples containing rhodamine and fluorescein were excited with light at 555 nm and 495 nm respectively. Fluorescence emission was measured between 515/565 nm and 700 nm, with excitation/emission slits set at 5.0 nm at a scan speed of 200 nm/min. Fluorescence anisotropy measurements (slit widths, 15.0 nm for excitation/emission) were made using the same experimental setup using a G-factor (GF) of 1 and an integration time of 2.0 seconds.

Polymerase Chain Reaction (PCR). All PCR reactions were carried out using a Biometra(R) T 3000 Thermocycler. 100 ng of pcDNA template was used in a final reaction volume of 50 μL. Reaction mixture included either the unconjugated **R-For** oligonucleotide or **R-For** conjugated to M13 bacteriophage and antisense oligonucleotide primers (2 pmol/μl); 200 μM dNTPs, 0.2 nmol/ul; GoTaq DNA polymerase (5 units) in 1x GoTaq Flexi Green buffer. 1.5 μL of ethylene glycol was added to the mixtures in order to allow for the amplification at lower temperatures. DNA was amplified using the following conditions: 86.0 °C for 5 min (preheating); denaturing 86.0 °C, 1 min; annealing 50.0 °C, extension 72.0 °C, 1 min. Repeat from denaturation 35 times. Followed by a final extension 72.0 °C for 5 minutes. Lid temperature was set at 86.0 °C.

Agarose Gel Electrophoresis. The PCR mixtures were run on a horizontal 1% (w/v) agarose gel using 2 × TAE buffer. Ethidium bromide was added to the gel before the gel had set to visualize the PCR product(s).

10 μL of each sample was loaded onto the gel in 2 × TAE buffer. A 1 kbp ladder DNA ladder was used as a reference. The gel was subsequently run at 80 V for 30 minutes, before being visualized on a light box.

ASSOCIATED CONTENT

Supporting Information.

Figures S1—S7 as well as Table S1 including sequence and conjugate characterization. This material is available free of charge via the Internet at http://pubs.acs.org.

AUTHOR INFORMATION

Corresponding Author

*Professor Timothy R. Dafforn. t.r.dafforn@bham.ac.uk,

*Professor James H. R. Tucker, j.tucker@bham.ac.uk

Present Addresses

[||]Nadja Steinke is currently at the TU - Institut für Lebensmittel- und Bioverfahrenstechnik, Dresden.

Author Contributions

[#]JC-S and RP-G contributed equally to this work and have shared first authorship. Names listed in alphabetical order. The manuscript was written through contributions of all authors.

Notes

The authors declare no competing financial interests.

ACKNOWLEDGMENT

We gratefully acknowledge the support provided by Dr. Jonathon Snelling and Dr. Chi Tsang for analytical support. JHRT acknowledges the EPSRC for the award of a Leadership Fellowship (EP/G007578/1). TRD thanks the BBSRC (BB/J02001X/1), and EPSRC (EP/I502025/1, EP/G005869/1, EP/G007578/1) for their support.

REFERENCES

[1] Thomson, A. R., Wood, C. W., Burton, A. J., Bartlett, G. J., Sessions, R. B., Brady, R. L., and Woolfson, D. N. (2014) Computational design of water-soluble α-helical barrels, *Science 346*, 485-488.

[2] Wood, C. W., Bruning, M., Ibarra, A. Á., Bartlett, G. J., Thomson, A. R., Sessions, R. B., Brady, R. L., and Woolfson, D. N. (2014) CCBuilder: An interactive web-based tool for building, designing and assessing coiled-coil protein assemblies., *Bioinformatics 30*, 3029-3035.

[3] Berwick, M. R., Lewis, D. J., Jones, A. W., Parslow, R. A., Dafforn, T. R., Cooper, H. J., Wilkie, J., Pikramenou, Z., Britton, M. M., and Peacock, A. F. A. (2014) De novo design of Ln(III) coiled coils for imaging applications., *J. Am. Chem. Soc. 136*, 1166-1169.

[4] Gribbon, C., Channon, K. J., Zhang, W., Banwell, E. F., Bromley, E. H. C., Chaudhuri, J. B., Oreffo, R. O. C., and Woolfson, D. N. (2008) Magicwand: A single, designed peptide that assembles to stable, ordered α-helical fibers, *Biochemistry 47*, 10365-10371.

[5] Pandya, M. J., Spooner, G. M., Sunde, M., Thorpe, J. R., Rodger, A., and Woolfson, D. N. (2000) Sticky-end assembly of a designed peptide fiber provides insight into protein fibrillogenesis, *Biochemistry 39*, 8728-8734.

[6] Bromley, E. H. C., Channon, K. J., King, P. J. S., Mahmoud, Z. N., Banwell, E. F., Butler, M. F., Crump, M. P., Dafforn, T. R., Hicks, M. R., Hirst, J. D., Rodger, A., and Woolfson, D. N. (2010) Assembly pathway of a designed alpha-helical protein fiber., *Biophys. J. 98*, 1668-1676.

[7] Bongiovanni, M. N., Scanlon, D. B., and Gras, S. L. (2011) Functional fibrils derived from the peptide ttr1-cyclorgdfk that target cell adhesion and spreading., *Biomaterials 32*, 6099-6110.

[8] Lakshmanan, A., Zhang, S., and Hauser, C. A. E. (2012) Short self-assembling peptides as building blocks for modern nanodevices., *Trends Biotechnol. 30*, 155-165.

[9] Ghosh, D., Bagley, A. F., Na, Y. J., Birrer, M. J., Bhatia, S. N., and Belcher, A. M. (2014) Deep, noninvasive imaging and surgical guidance of submillimeter tumors using targeted M13-stabilized single-walled carbon nanotubes., *Proc. Natl. Acad. Sci. U. S. A. 111*, 13948-13953.

[10] Oh, D., Qi, J., Han, B., Zhang, G., Carney, T. J., Ohmura, J., Zhang, Y., Shao-Horn, Y., and Belcher, A. M. (2014) M13 virus-directed synthesis of nanostructured metal oxides for lithium-oxygen batteries., *Nano Lett. 14*, 4837-4845.

[11] Chen, P.-Y., Dang, X., Klug, M. T., Qi, J., Dorval Courchesne, N.-M., Burpo, F. J., Fang, N., Hammond, P. T., and Belcher, A. M. (2013) Versatile three-dimensional virus-based template for dye-sensitized solar cells with improved electron transport and light harvesting., *ACS Nano 7*, 6563-6574.

[12] Brasino, M., Lee, J. H., and Cha, J. N. (2014) Creating highly amplified enzyme-linked immunosorbent assay signals from genetically engineered bacteriophage, *Anal. Biochem. 470*, 7-13.

[13] Domaille, D. W., Lee, J. H., and Cha, J. N. (2013) High density DNA loading on the M13 bacteriophage provides access to colorimetric and fluorescent protein microarray biosensors., *Chem. Commun. 49*, 1759-1761.

[14] Lee, J. H., Domaille, D. W., and Cha, J. N. (2012) Amplified protein detection and identification through DNA-conjugated M13 bacteriophage., *ACS Nano 6*, 5621-5626.

[15] Clack, B. A., and Gray, D. M. (1992) Flow linear dichroism spectra of four filamentous bacteriophages: DNA and coat protein contributions, *Biopolymers 32*, 795-810.

[16] Hicks, M. R., Rodger, A., Lin, Y.-p., Jones, N. C., Hoffmann, S. V., and Dafforn, T. R. (2012) Rapid injection linear dichroism for studying the kinetics of biological processes., *Anal. Chem. 84*, 6561-6566.

[17] Pacheco-Gómez, R., Kraemer, J., Stokoe, S., England, H. J., Penn, C. W., Stanley, E., Rodger, A., Ward, J., Hicks, M. R., and Dafforn, T. R. (2012) Detection of pathogenic bacteria using a homogeneous immunoassay based on shear alignment of virus particles and linear dichroism, *Anal. Chem. 84*, 91-97.

[18] Hess, G. T., Guimaraes, C. P., Spooner, E., Ploegh, H. L., and Belcher, A. M. (2013) Orthogonal labeling of M13 minor capsid proteins with DNA to self-assemble end-to-end multiphage structures., *ACS Syn. Bio. 2*, 490-496.

[19] Chrisey, L. A., Lee, G. U., and Ferrall, C. E. (1996) Covalent attachment of synthetic DNA to self-assembled monolayer films., *Nucleic Acids Res. 24*, 3031-3039.

[20] Kuijpers, W. H. A., Kaspersen, F. M., Veeneman, G. H., Van Boeckel, C. A. A., and Bos, E. S. (1993) Specific recognition of antibody-oligonucleotide conjugates by radiolabeled antisense nucleotides: A novel approach for two-step radioimmunotherapy of cancer, *Bioconjugate Chem. 4*, 94-102.

[21] Li, K., Chen, Y., Li, S., Nguyen, H. G., Niu, Z., You, S., Mello, C. M., Lu, X., and Wang, Q. (2010) Chemical modification of M13 bacteriophage and its application in cancer cell imaging, *Bioconjugate Chem. 21*, 1369-1377.

[22] McLachlan, J. R. A., Smith, D. J., Chmel, N. P., and Rodger, A. (2013) Calculations of flow-induced orientation distributions for analysis of linear dichroism spectroscopy, *Soft Matter 9*, 4977-4984.

[23] Halsall, D. J., Rodger, A., and Dafforn, T. R. (2001) Linear dichroism for the detection of single base pair mutations, *Chem. Commun.*, 2410-2411.

[24] Nordén, B., Rodger, A., and Dafforn, T. (2010) *Linear dichroism and circular dichroism*, Royal Society of Chemistry.

[25] Jahn, T. L., Lanoman, M. D., and Fonseca, J. R. (1964) The mechanism of locomotion of flagellates. II. Function of the mastigonemes of ochromonas*, *The Journal of Protozoology 11*, 291-296.

[26] Holwill, M. E., and Sleigh, M. A. (1967) Propulsion by hispid flagella, *J. Exp. Biol. 47*, 267-276.

[27] Nguyen, H. V., Zhao, Z.-y., Sallustrau, A., Horswell, S. L., Male, L., Mulas, A., and Tucker, J. H. R. (2012) A ferrocene nucleic acid oligomer as an organometallic structural mimic of DNA., *Chem. Commun. 48*, 12165-12167.

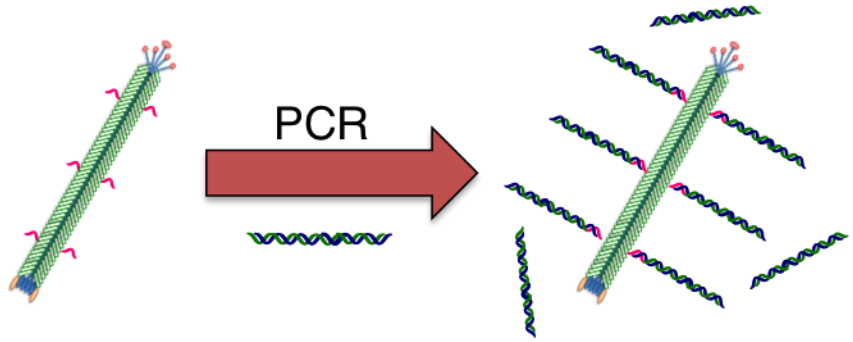
PCR